Electronic Supplementary Information:

V_2O_5 Cathode for Aqueous Rocking-chair Pb-ion Batteries

Ningbo Liu, Xiaoying Zhao, Xiaohan Wang, Qiaqia Li and Liubin Wang*

College of Chemistry & Materials Science, Key Laboratory of Analytical Science and Technology of Hebei Province, Hebei University, Baoding 071002, China

E-mail address: lbwang@hbu.edu.cn.

1.Experimental Section

***Material Synthesis*:**1.2 g of commercial V_2O_5 and 2.4 g of $H_2C_2O_4 \cdot 2H_2O$ were dissolved in 40 mL of deionized water and vigorously stirred at 90 °C for 5 h to form a blue solution. Then, 8 mL of H_2O_2 (35 wt %) was added to the blue solution followed by stirring for 30 min. 100 ml of ethanol was then added into the mixture and stirred for 1 h. The formed dark-green mixture was subsequently loaded into a 200 mL autoclave with a Teflon liner and held at 170 °C for 12 h. After the reaction, the precipitate was collected and thoroughly washed with deionized water and ethanol and dried at 60 °C for 12 h. Finally, the precipitation was calcined in 450 ℃ air for 3 h to obtain anhydrous V_2O_5.

***Electrochemical Measurements*:** The as-prepared V_2O_5 powder, poly(1,1-difluoroethylene) (PVDF), and Super P were mixed in solid form in a mass ratio of 7:2:1. N-Methylpyrrolidone (NMP) solvent was added into the solid mixture and stirred for 1 h to form a homogeneous slurry. The slurry was uniformly coated on a Titanium sheet (1.1304 cm^2) and dried at 70 °C for 8 h in a vacuum. The mass loading of the active materials per Titanium sheet is 1.0-1.5 mg cm^{-2}.

***Electrolyte Characterization*:** The Pb plating/stripping process in the electrolyte was indicated by CV curves at a scan rate of 2.0 mV s^{-1}, which was tested on a CHI760 electrochemical workstation. Titanium foil is used as the current collector. CR2032 coin cells were assembled using pure Pb as the counter electrode, the active material as the working electrode, and the filter paper as separators. The electrolyte was 1.0 M $Pb(AC)_2$. Galvanostatic tests were carried out with a voltage range of 0.1-1.2 V (vs. Pb^{2+}/Pb) on the LAND battery tester (CT3001A). The galvanostatic intermittent titration technique (GITT) measurements were performed at 10 mA g^{-1} with a charge/discharge of 10 min and a relaxation time under the open circuit potential of 40 min.

***Materials characterization*:** X-ray diffraction (XRD) patterns of the samples were recorded by the Bruker D8 Advance diffractometer with Cu Kα radiation from 5° to 80° at a sweep rate of 4° min^{-1} to identify the crystal structure. Scanning electron microscopy (SEM, Nova NanoSEM450) and Transmission electron microscope (TEM, JEOL JEM-2100Plus) were used to observe the crystal morphologies and microstructures with elemental mapping. The spectroscopic characteristics of the samples were acquired by using Raman spectroscopy (Raman, HORIBA, LabRAM HR Evolution) with a laser wavelength of 532 nm, Fourier transform infrared spectroscopy (Thermo Scientific Nicolet iS 10 spectrometer), and X-ray photoelectron spectroscopy (XPS, PHI 1600 ESCA, Perkin-Elmer).

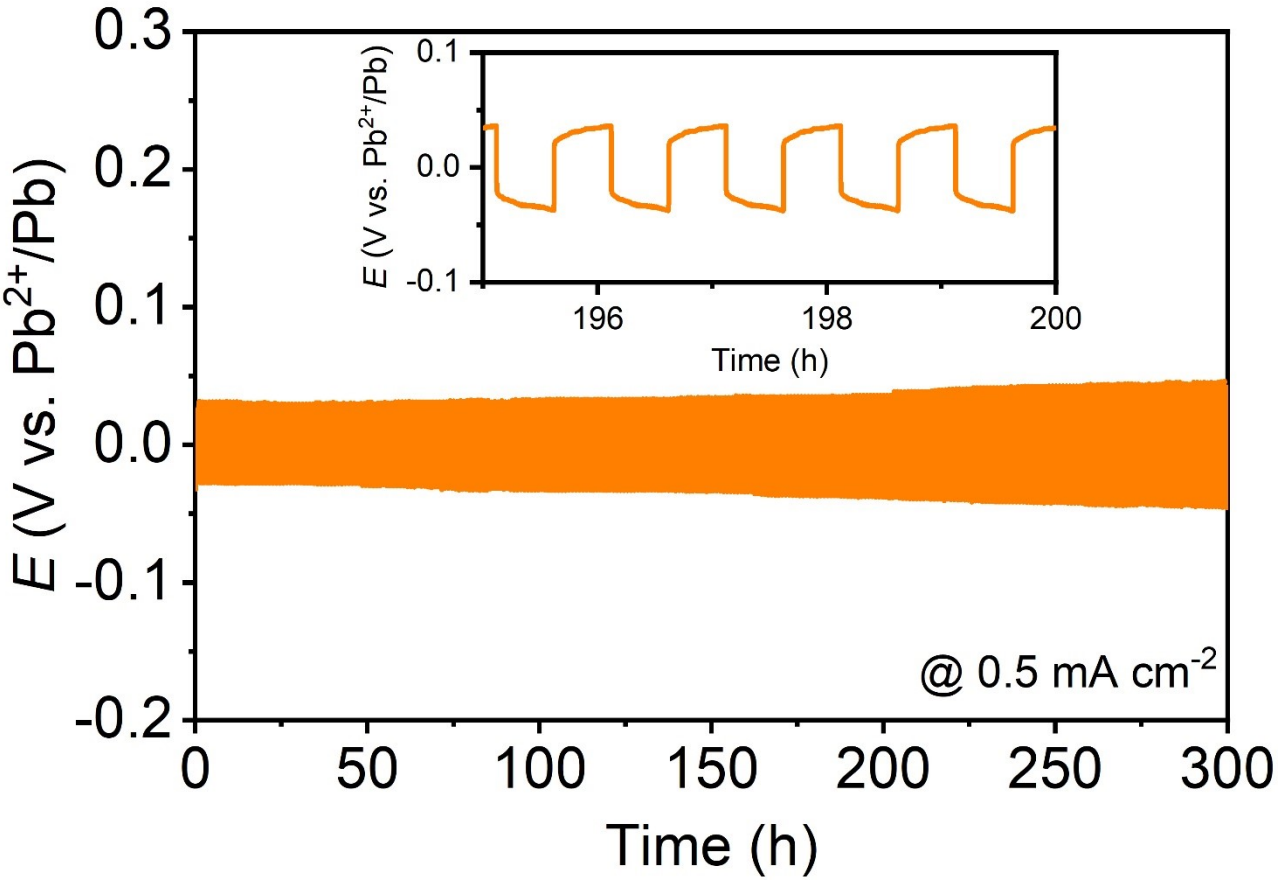

Fig. S1. Cycling performances of a symmetrical Pb/Pb coin cell at a current density of 0.5 mA cm^{-2}, where one sweep of plating or stripping process lasts for 0.5 h.

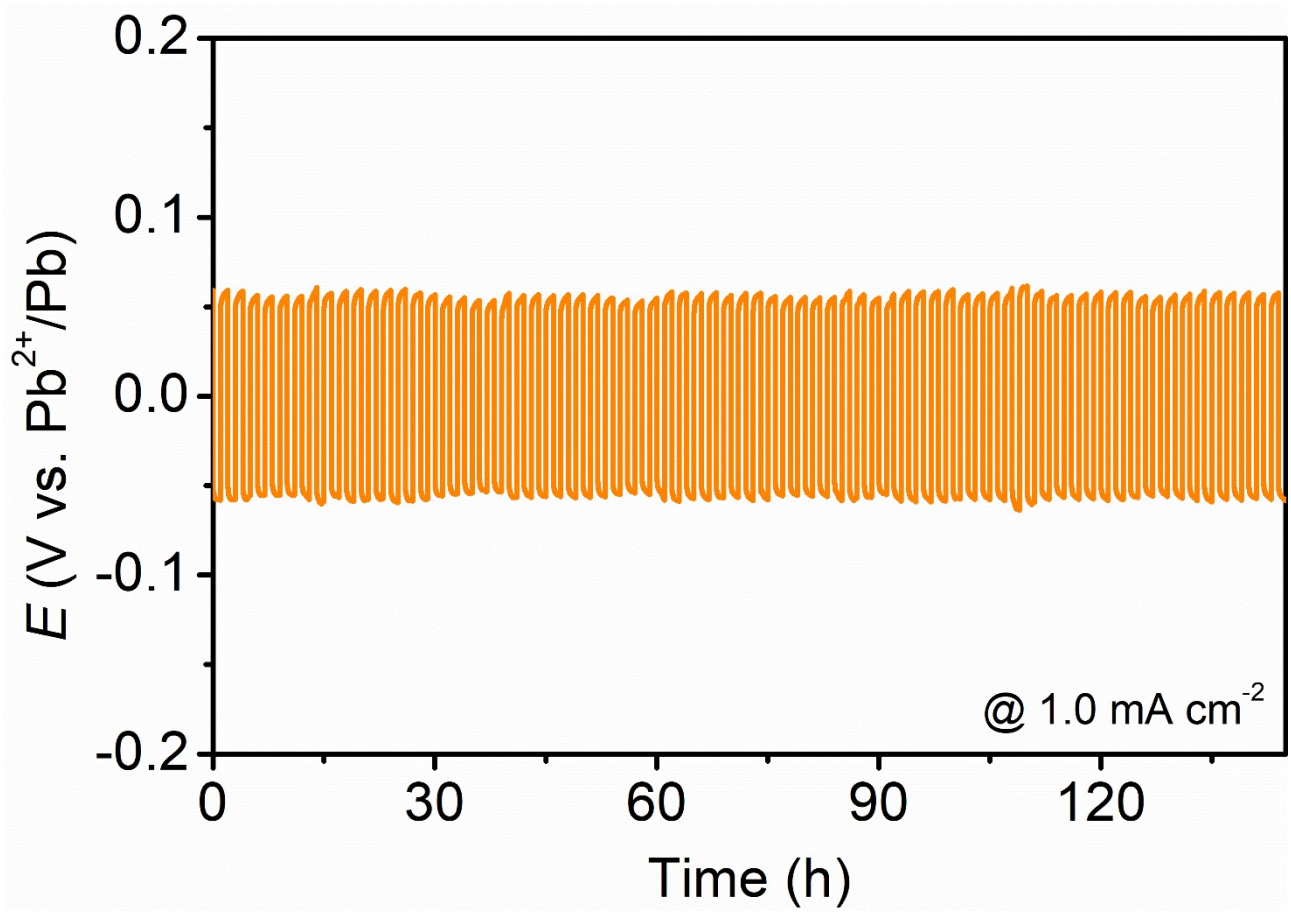

Fig. S2. Cycling performances of a symmetrical Pb/Pb coin cell at a current density of 1.0 mA cm^{-2} with 1.0 mAh cm^{-2}.

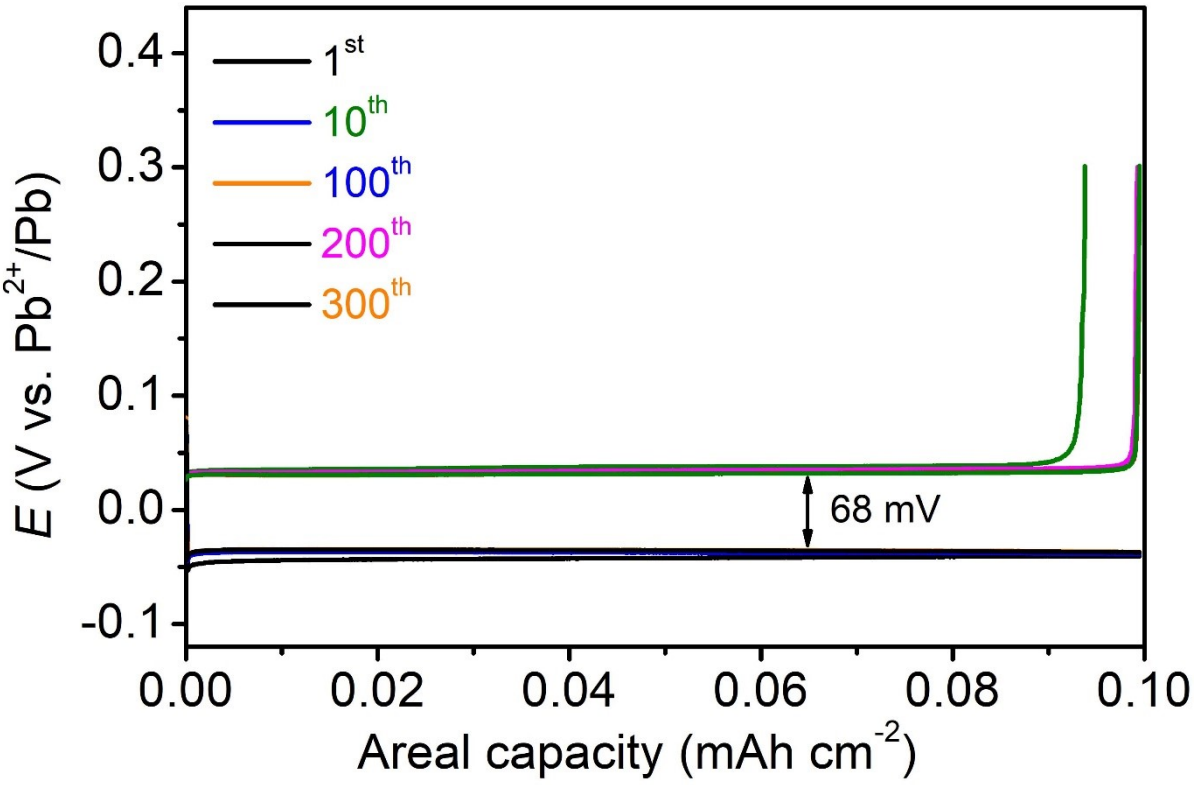

Fig. S3. Voltage profiles of an asymmetrical Pb/Cu coin cell at a current density of 0.2 mA cm^{-2} for 0.5 h.

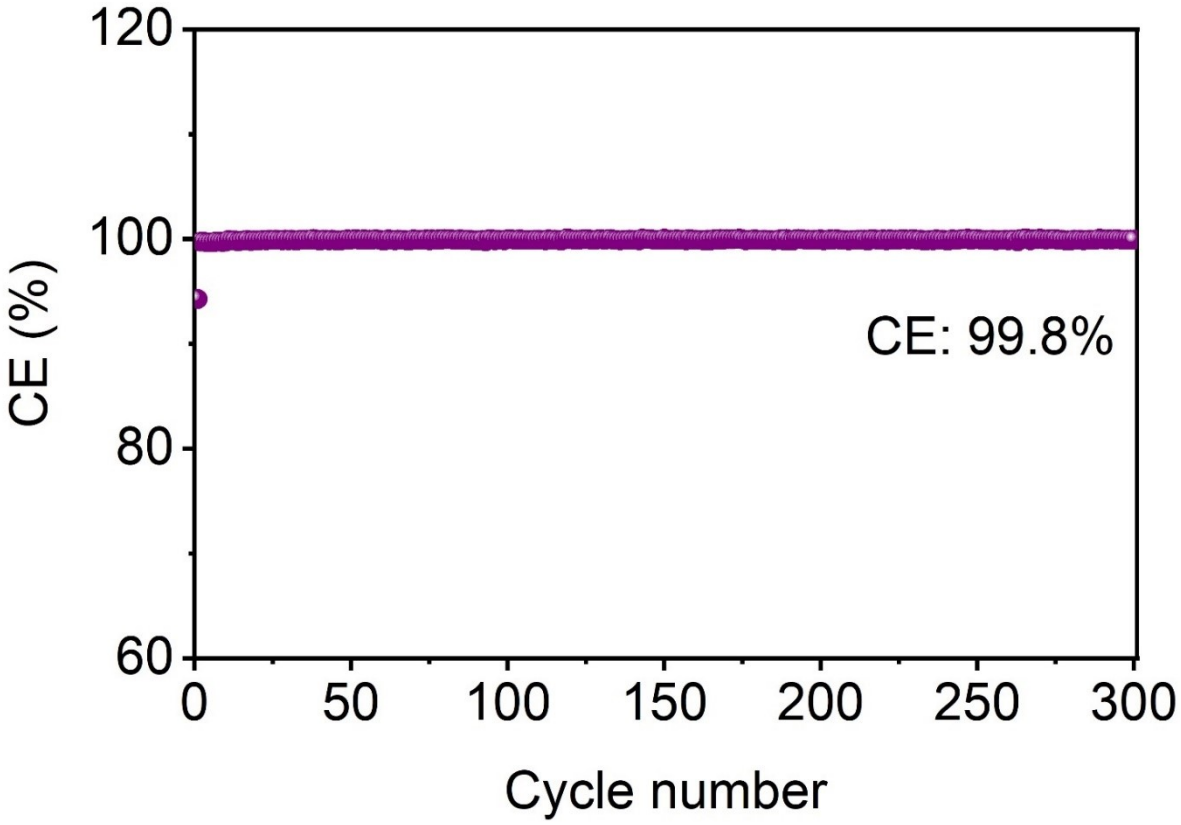

Fig. S4. CE values of Pb plating/stripping in the Pb/Cu asymmetrical cell.

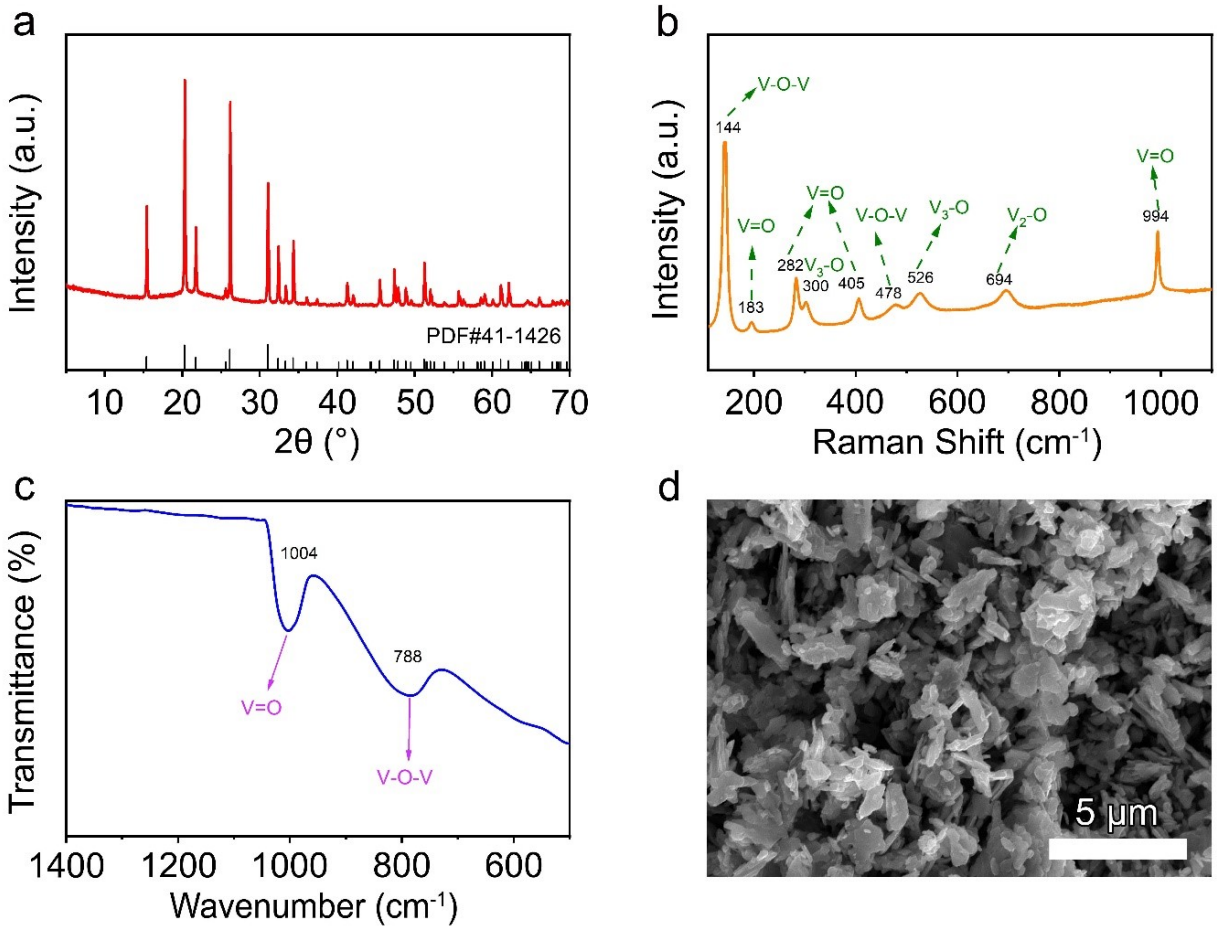

Fig. S5. (a) XRD patterns of V_2O_5, (b) Raman, (c) FTIR and (d) SEM image.

Fig. S5a shows the X-ray diffraction (XRD) patterns of the as-prepared V_2O_5. Where all the characteristic peaks are well indexed to the standard pattern of orthorhombic V_2O_5 (space group of Pmn21, JCPDS No.41–1426). The molecular Vibration information of V_2O_5 was carried out to characterize by Raman spectra (Fig. S5b). The strong band at 144 cm^{-1} is assigned to the skeleton bending vibration of V-O-V bond. The peaks at 183, 282 and 405 cm^{-1} correspond to the bending vibrations of V=O bonds. The peaks locating at 300 and 526 cm^{-1} are indexed to the bending vibrations and stretching modes of V_3-O (triply coordinated oxygen) bonds, respectively. The peaks at 478 $cm^{-1}$is assigned to the bending vibrations of the V-O-V bonds (bridging doubly coordinated oxygen). The band at 694 cm^{-1} is corresponding to stretching mode of the doubly coordinated oxygen (V_2-O). The band at 989 cm^{-1} is attribute to the stretching vibrational mode of the apical V=O bond (terminal oxygen). [S1-S3] According to FTIR spectra (Fig. S5c), the characteristic bands at 788 cm^{-1} is attributed to the vibration of V_3-O while the absorption peak at 1004 cm^{-1} is related to stretching vibration of V=O bands. [S4] The scanning electron microscopy (SEM) shows that V_2O_5 is mainly constructed with short nanorods in Fig. S5d.

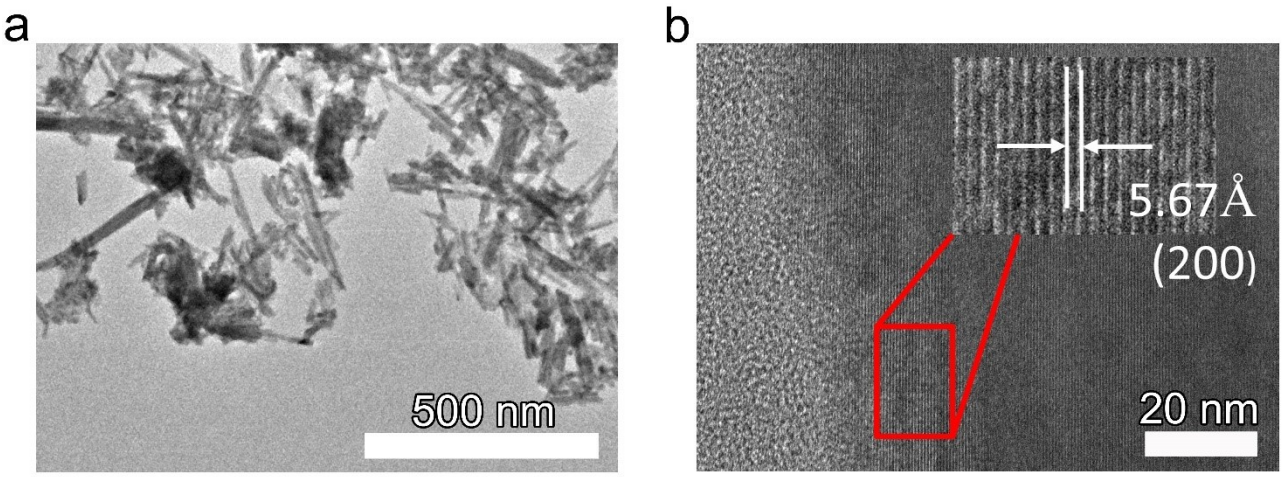

Fig. S6. TEM and high-resolution TEM images.

The high-resolution TEM image displays a lattice spacing of 5.67Å, which corresponds to the spacing of (200) plane of V_2O_5.

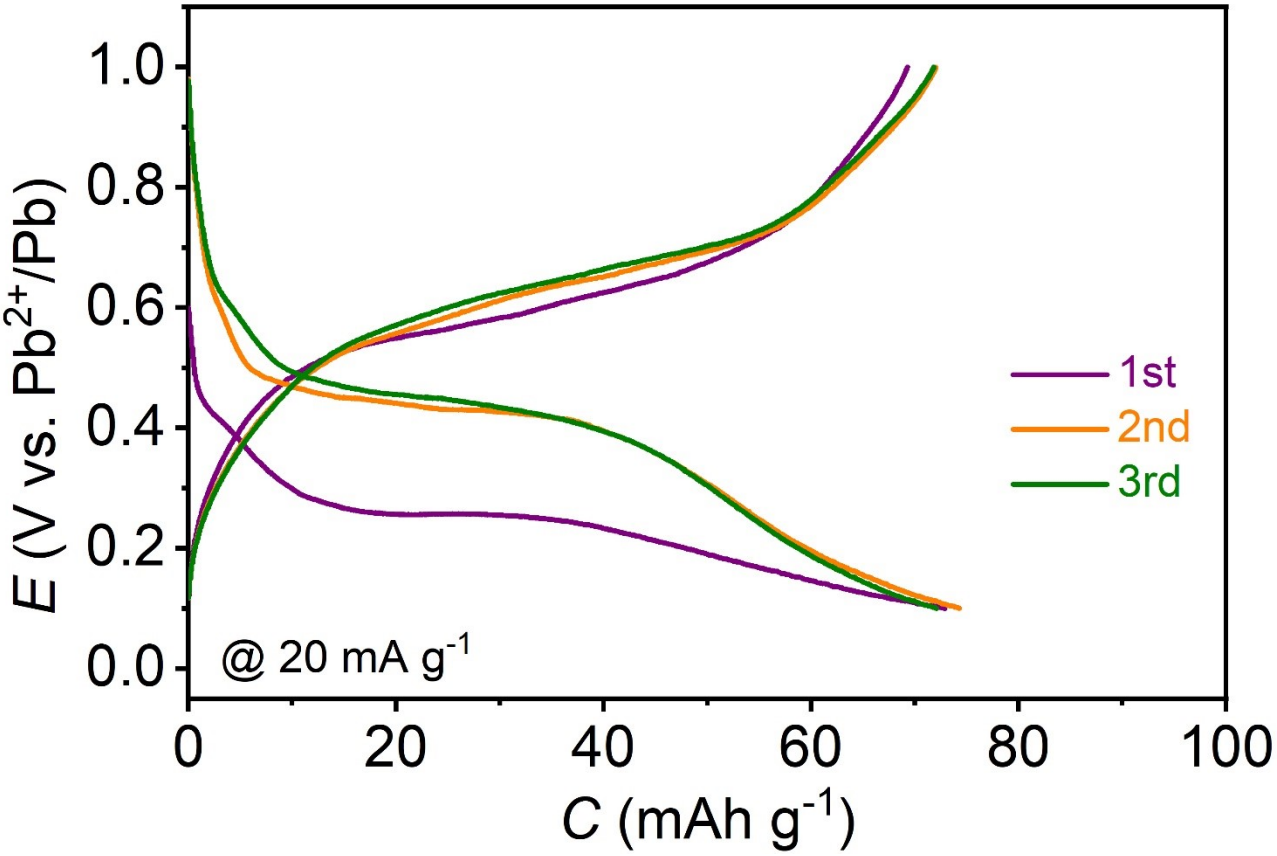

Fig. S7. Galvanostatic charge/discharge characterization curves of the Pb/V_2O_5 battery at 20 mA g^{-1} in 1M $Pb(ClO_4)_2$ electrolyte.

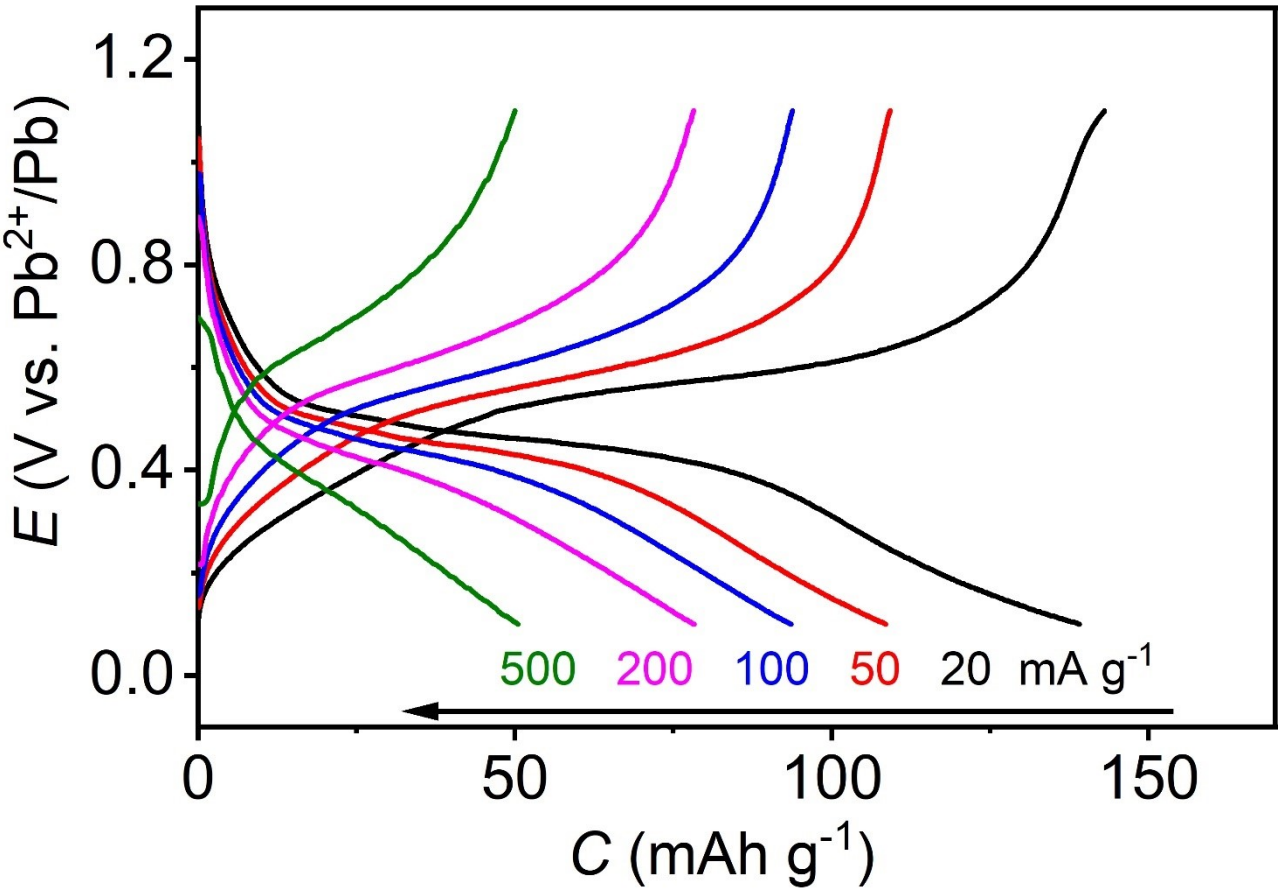

Fig. S8. The corresponding discharge/charge curves at different current densities.

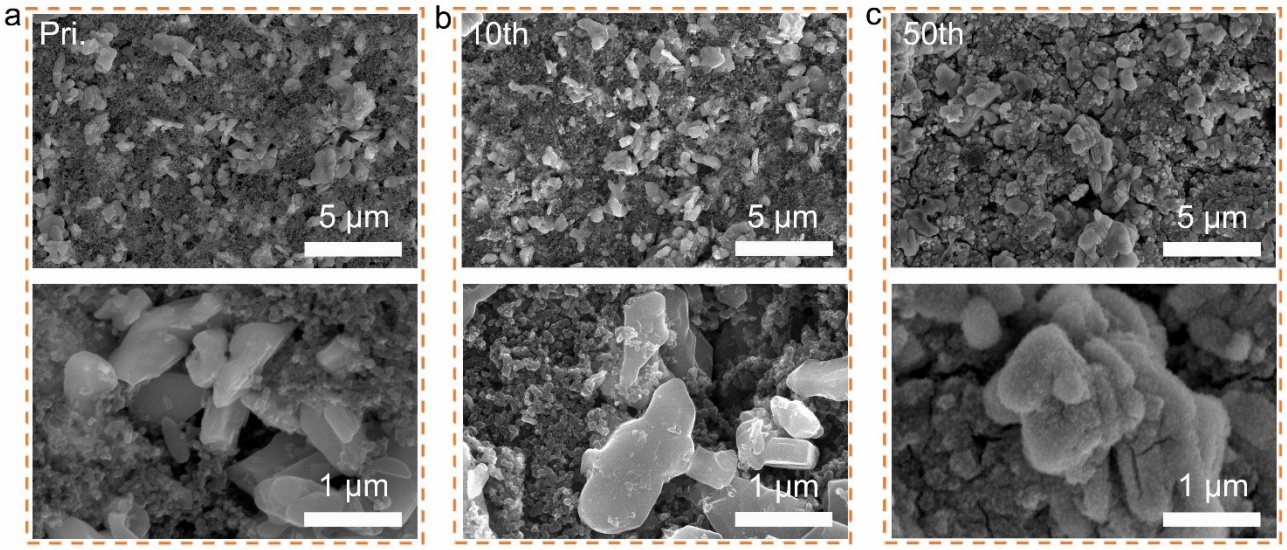

Fig. S9. SEM images of V_2O_5 electrode at (a) pristine state, (b) 10 cycles, and (c) 50 cycles.

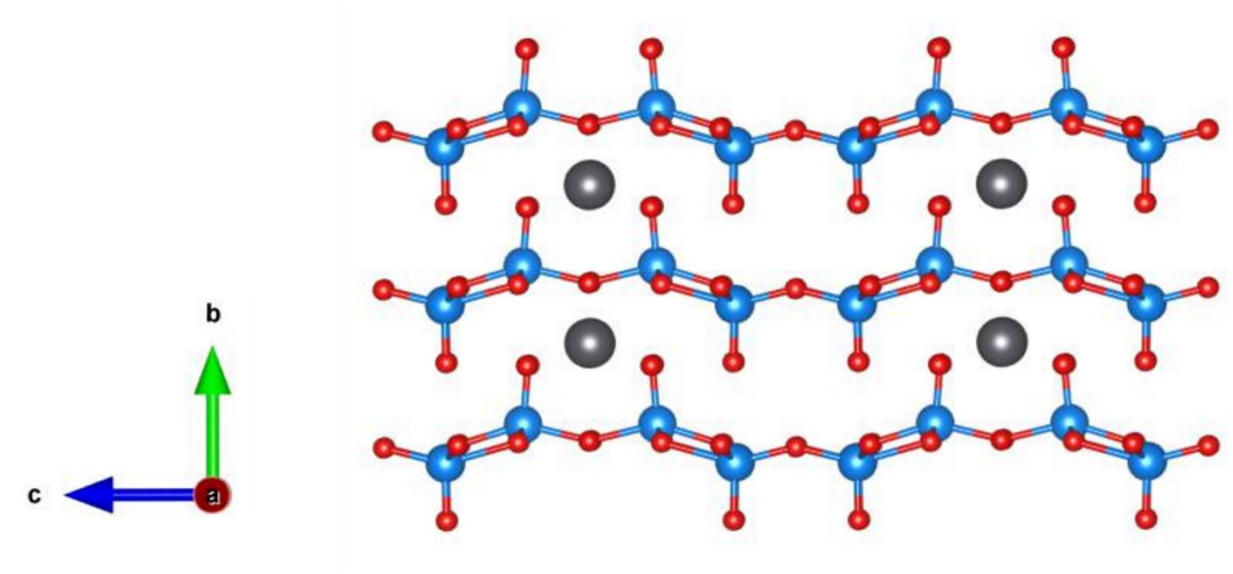

Fig. S10. Crystal structure of $Pb_{0.5}V_2O_5$. (a=3.68146 Å，b=4.41826 Å，c=11.53896 Å，α=γ=β=90.0000°, V=187.6887 $Å^3$)

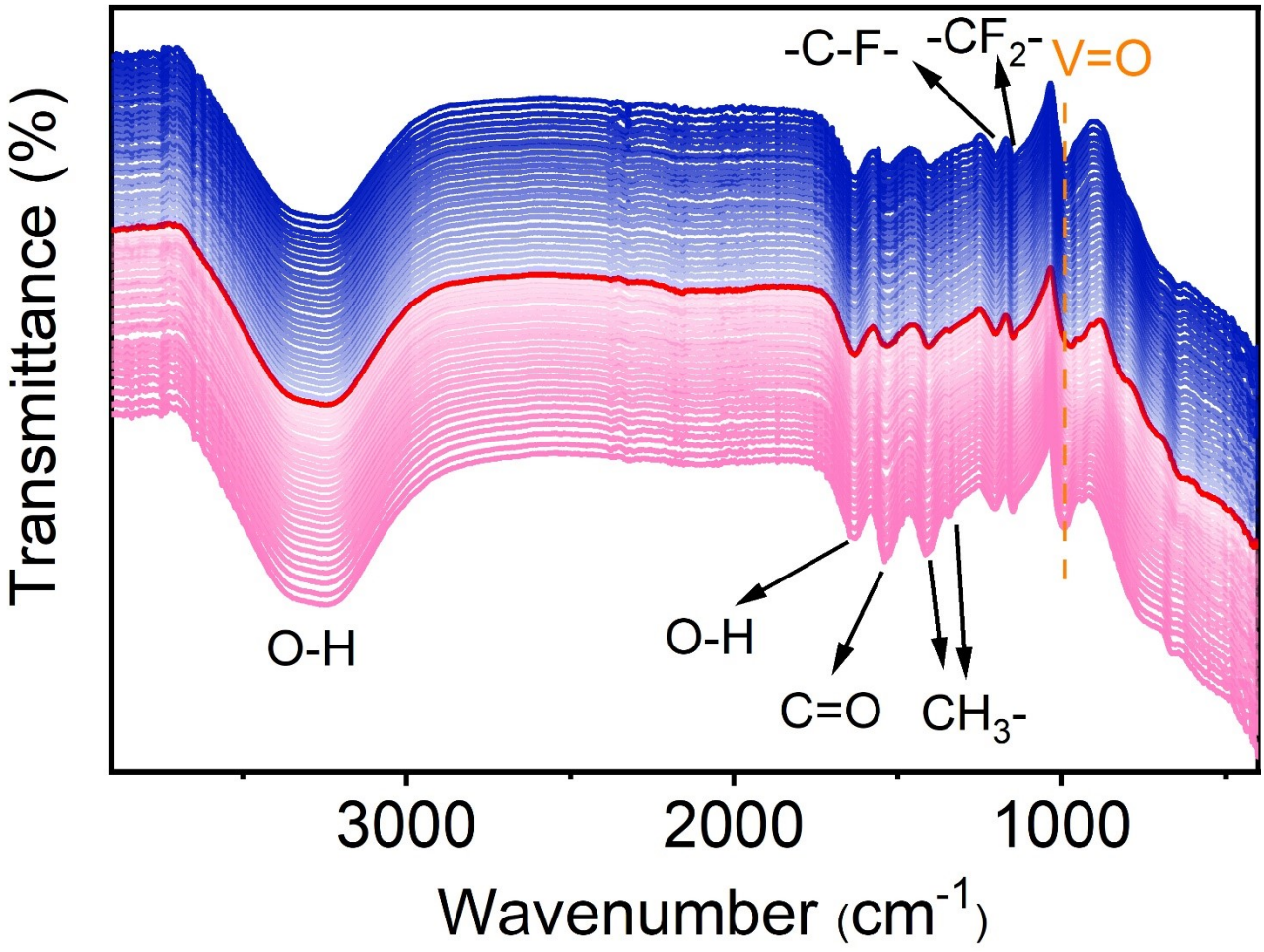

Fig. S11. Full spectrum of in-situ FTIR during charge/discharge process.

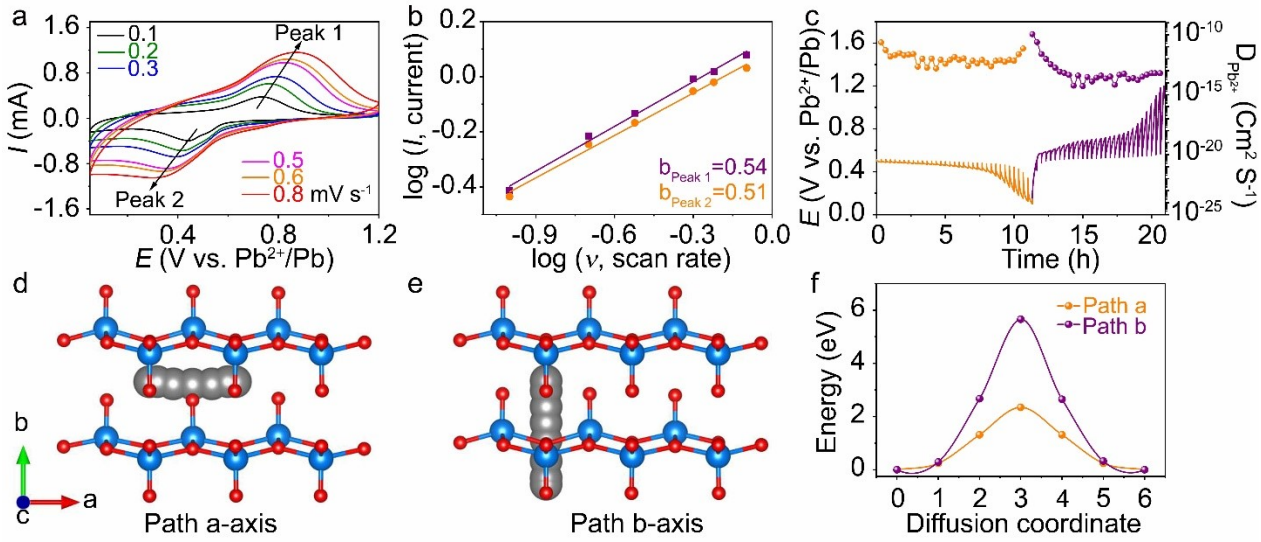

Fig. S13. (a) CV curves at different scan rates, (b) log (*i*, current) vs. log (*v*, scan rate) plots, (c) GITT curves and calculated Pb^{2+} diffusion coefficients of V_2O_5, (d, e) Pb^{2+} diffusion behaviors along the a-axis and b-axis in V_2O_5 lattice simulated by DFT computations, (f) Comparison of diffused energy barriers of path a and path b.

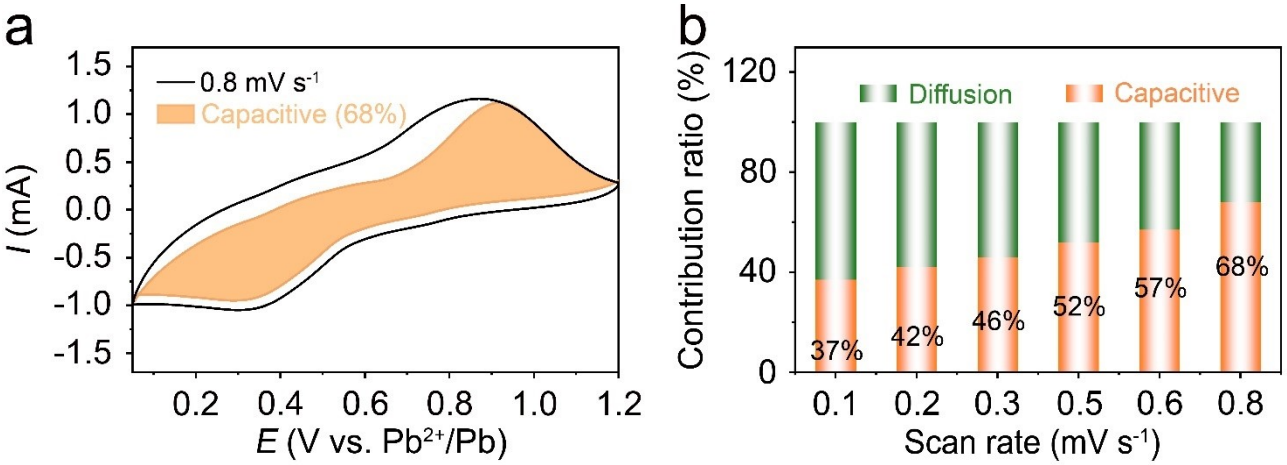

Fig. S13. (a) Capacitance separation at 0.8 mV s^{-1} for the V_2O_5 electrodes, (b) Capacitive contribution of V_2O_5 at various scan rate.

The capacitance (k_1v) and intercalation ($k_2v^{1/2}$) contributions are quantified based on the equation of $i(V) = k_1v + k_2v^{1/2}$.

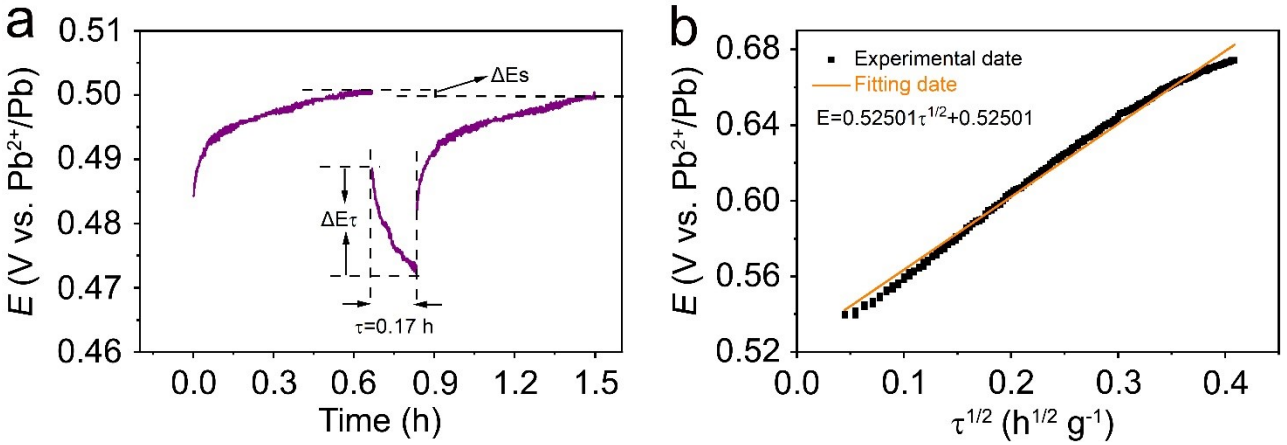

Fig. S14. (a) Current step diagram of the GITT curves and (b) Liner fit of the transient potential changes (E) vs ($\tau^{1/2}$).

In our study, the current pulse lasted for 10 min at 10 mA g^{-1} and then the cell was relaxed for 40 min to make the voltage reach the equilibrium. These procedures were repeatedly applied to the cell during the entire discharge/charge process. The Pb^{2+} diffusion coefficients in the V_2O_5 cathode were calculated from the GITT data by following formula[S5]:

$$D_{GITT} = \frac{4}{\pi}\left(\frac{m_B V_m}{M_B S}\right)^2\left(\frac{\Delta E_s}{\tau(dE_\tau/d\sqrt{\tau})}\right)^2 \approx \frac{4}{\pi\tau}\left(\frac{m_B V_m}{M_B S}\right)^2\left(\frac{\Delta E_s}{\Delta E_\tau}\right)^2\left(\tau \ll \frac{L^2}{D_{GITT}}\right)$$

Where D_{Pb2+} ($cm^2\ s^{-1}$) means the chemical diffusion coefficient, τ is the constant current duration time (10 min), m_B is the mass of active material, M_B is the molecular weight (g mol^{-1}) and V_m is its molar volume ($cm^3\ mol^{-1}$), S is the total contacting area of electrode with electrolyte (1.1304 cm^2), and ΔE_s and ΔE_τ are the change in the steady state voltage and overall cell voltage after the application of a current pulse in a single step GITT experiment, respectively. As indicated in Fig. S10b, the cell voltage as a function of $\tau^{1/2}$ shows a linear relationship.

References

S1. B. Yan, L. Liao, Y. You, X. Xu, Z. Zheng, Z. Shen, J. Ma, L. Tong, T. Yu, *Adv. Mater.*, 2009, **21**, 2436-2440.

S2. Y. Song, T. Y. Liu, B. Yao, T. Y. Kou, D. Y. Feng, X. X. Liu, Y. Li, *Small*, 2017, **13**, 1700067.

S3. D. Zhao, X. Wang, W. Zhang, Y. Zhang, Y. Lei, X. Huang, Q. Zhu, J. Liu, *Adv. Funct. Mater.*, 2023, **33**, 2211412.

S4. S. Chen, K. Li, K. S. Hui, J. Zhang, *Adv. Funct. Mater.*, 2020, **30**, 2003890.

S5. L. Wang, C. Wang, N. Zhang, F. Li, F. Cheng, J. Chen, *ACS Energy Lett.*, 2017, **2**, 256-262.